FIGURE 66.—Part a: Distribution of Fischer-Tropsch Products According to Carbon Number (Tests of Cobalt Catalysts at Atmospheric Pressure and About 190°); part b: Probability That a Hydrocarbon Radical on Surface Will Appear as Product of Chain Length n Rather Than Grow to Higher Molecular Weight.

TABLE 65.—*General olefin types, C_6-C_8, volume-percent*

Fraction	α-olefins	Internal double-bond olefins	
		Trans	Cis
C_6	36 ± 2	39 ± 3	25 ± 3
C_7	28 ± 2	42 ± 5	30 ± 5
C_8	18 ± 2	52 ± 5	30 ± 5

Herington [11] considered the formation of hydrocarbons by one-carbon-atom additions to a hydrocarbon chain growing at the catalyst surface, assuming that hydrocracking reactions are not important. He defined a quantity β_n, the probability that a hydrocarbon chain of length n on the catalyst will appear as product of length n divided by the probability of growing at the surface to appear in the products as a hydrocarbon of greater chain length, by equation (30).

$$\beta_n = \phi_n \Big/ \sum_{n+1}^{\infty} \phi_i, \tag{30}$$

where ϕ_i is the number of moles of hydrocarbons of length i in the product.

Further consideration of Herington's approach leads to

$$\beta_n = (1-\alpha_n)/\alpha_n \text{ or } \alpha_n = (1+\beta_n)^{-1}, \tag{31}$$

where α_n is the probability of growth of a chain of length n. It can be shown that for any range of constant value of β_n

$$\phi_{n+1} = \phi_n(1+\beta)^{-1} = \phi_n \alpha, \tag{32}$$

and

$$\phi_n = \phi_x \alpha^{n-x} \tag{33}$$

Also

$$W_n \cong 14 n \phi_x \alpha^{n-x}, \tag{34}$$

where W_n is the weight of hydrocarbons of carbon number n. The weight-distribution curve of equation (34) exhibits a maximum at $n = -1/\log_e \alpha$, but the mole-distribution curve (equation (33)) decreases monotonically. A plot of $\log \phi_n$ against n (equation (33)) should be linear.

Figure 66, part b, presents a plot of β_n for the data of figure 66, part a. For the range C_5 to C_{15} the value of β_n is approximately 0.2 ($\alpha_n = 0.83$). This value differs considerably from that found by Herington, where β_n was about 0.3 ($\alpha_n = 0.77$) and reflects the differences in the distribution curves. For $\beta = 0.2$ a maximum in the weight distribution is predicted at

[11] Work cited in footnote 5, p. 112.

$n = 5$, while for $\beta = 0.3$ the maximum is predicted at $n = 4$.

A plot of most of the available carbon-number data for cobalt catalysts [12-16] according to equation (33) in figure 67 shows that the equation is a good approximation for both hydrocarbons and alcohols for $n > 2$. All of the plots, except that for the data of Friedel and Anderson, have essentially the same slope, corresponding to $\alpha = 0.75$. The reason for this exception is not apparent, since very similar catalysts were used in all experiments. The only significant difference is that the Bureau of Mines tests were made with pelleted catalysts whereas granular (broken filter cake) preparations were used in the other synthesis experiments.

Less detailed data are available for iron catalysts. Friedel and Anderson [17] reported preliminary results indicating that less paraffins are formed. The distribution of gaseous products from iron catalysts, shown in table 66, indicates a minimum of C_2 products which was less pronounced than that observed for products from cobalt catalysts. Sizable amounts of ethylene were formed, and the olefins in the C_3, C_4, and C_5 hydrocarbons exceeded 70 percent. The olefin content in the C_6-C_9 portion is also high, being approximately 2.5 times greater than in liquids from cobalt catalysts. Olefins from the iron product are predominantly alpha rather than internal double-bond olefins. Some evidence has shown that chain branching in the olefins is nearly the same as that of the paraffins. The amount of material strongly adsorbed on silica gel (oxygenated compounds, aromatics,

TABLE 66.—*Gaseous products from iron catalysts* [1]

	Catalysts	Fused Fe₃O₄-MgO-K₂O Fe:MgO:K₂O= 100:6.8:0.83	Precipitated Fe₂O₃-CuO-K₂CO₃ Fe:Cu:K₂CO₃= 100:10:0.5
Hydrocarbon products.	C_1 gm./m.³	13.8	6.2
	C_2 { gm./m.³	8.6	5.6
	{ olefin, percent.	22.1	41.0
	C_3 { gm./m.³	14.3	8.7
	{ olefin, percent.	76.8	82.4
	C_4 { gm./m.³	8.0	2.7
	{ olefin, percent.	79.4	77.4
	C_5 olefin, percent.	77.7	72.0

[1] Tests were made with 1H₂:1CO gas at 7.8 atmospheres and space velocity of 100. Average temperatures of testing of fused catalyst and precipitated catalyst were 260° and 235°. Fused catalyst was reduced in hydrogen at 450° before use, and precipitated catalyst was inducted in 1H₂:1CO gas at 235° and atmospheric pressure.

[12] Work cited in footnote 4, p. 112.
[13] Work cited in footnote 5, p. 112.
[14] Ruhrchemie, A. G., Sterkrade-Holten: TOM reel 45, bag 3441, item 76.
[15] Ward, C. C., Schwartz, F. G., and Adams, N. G., Composition of Fischer-Tropsch (Cobalt Catalyst) Diesel Fuel: Ind. Eng. Chem., vol. 43, 1951, pp. 1117-1119.
[16] Gall, D., Gibson, F. J., and Hall, C. C., Distribution of Alcohols in the Products of the Fischer-Tropsch Synthesis: Jour. Appl. Chem. (London), vol. 2, 1952, pp. 371-380.
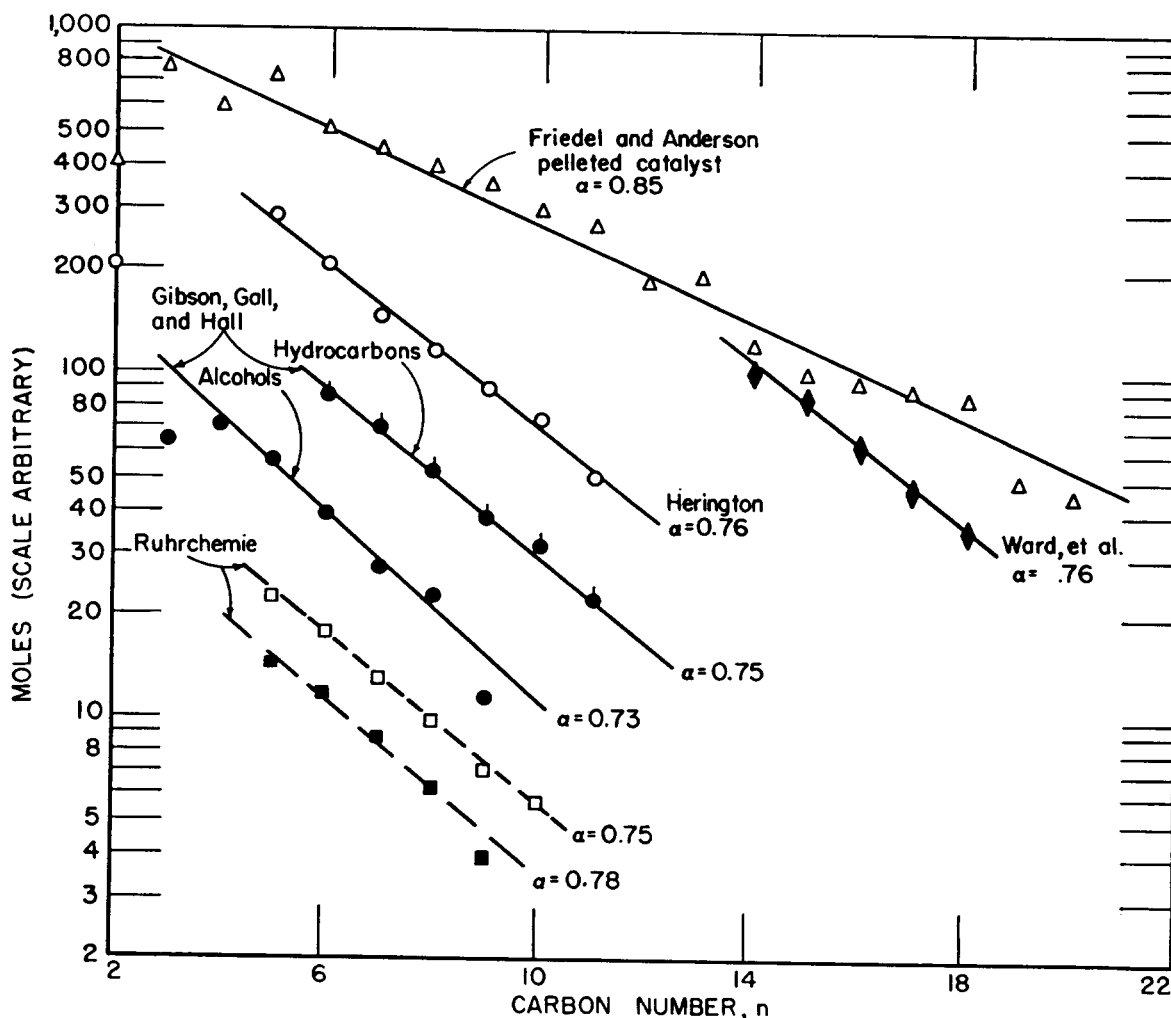[17] Work cited in footnote 4, p. 112.

FIGURE 67.—Semilogarithmic Carbon-Number Distribution Curves for Hydrocarbons and Alcohols From Normal-(Open Symbols) and Medium-(Solid Symbols) Pressure Syntheses With Cobalt Catalysts.

Data for hydrocarbons unless otherwise indicated.

etc.) is roughly three times as great in iron-catalyst products as from cobalt catalysts.

Carbon-number and olefin distributions from iron catalysts are available in reports of the Schwarzheide experiments.[18] These data plotted according to equation 33 in figure 68 show that the plots may be approximated by two straight lines, the first from n to 3 to 9 or 10 and the second for $n > 11$. The olefin content of products from iron catalysts (fig. 69) in some instances decreased with carbon number above C_2 and in others remained essentially constant.

Detailed analyses of products from the fluidized synthesis with iron catalysts have been presented by Bruner[19] and Weitkamp and co-workers.[20]

Manes[21] transformed equation (34) into a form that can be applied to the usual rough separations used to characterize the products from routine synthesis tests. This method provides a way of determining the value of α (an average value in the case of products from iron catalysts) that is useful in characterizing products in terms of one number. The total weight of the product that contains x or more carbon atoms per molecule may be expressed as

$$W_{x+} \cong 14\phi_x \sum_{n-x}^{\infty} n\alpha^{n-x}. \tag{35}$$

For α less than 1, equation (35) becomes

$$W_{x+} \cong 14\phi_x[x-\alpha(x-1)]/(1-\alpha)^2. \tag{36}$$

[18] TOM Reel 33, Schwarzheide Tests: Bag 3440, item 29.
[19] Bruner, F. H., Quality of Synthetic Gasoline From Natural Gas: Ind. Eng. Chem., vol. 41, 1949, pp. 2511-2515.
[20] Weitkamp, A. W., Seelig, H. S., Bowman, N. J., and Cady, W. E., Products of the Hydrogenation of Carbon Monoxide Over an Iron Catalyst; Aliphatic and Alicyclic Hydrocarbons: Ind. Eng. Chem., vol. 45, 1953, pp. 343-349; Cady, W. E., Launer, P. L., and Weitkamp, A. W.,

Aromatic Hydrocarbons: Pp. 350-353; Steitz, A., and Barnes, D. K., Water-Soluble Oxygenated Chemicals: Pp. 353-358; Cain, D. G., Weitkamp, A. W., and Bowman, N. J., Oil-Soluble Oxygenated Compounds: Pp. 359-362; Weitkamp, A. W., and Frye, C. G., Relation of Product Composition to Reaction Mechanism: Pp. 363-367.
[21] Manes, M., The Distribution of Liquid and Solid Fischer-Tropsch Hydrocarbons by Carbon Number: Jour. Am. Chem. Soc., vol. 74, 1952, pp. 3148-3151.

116   SYNTHETIC LIQUID FUELS FROM HYDROGENATION OF CARBON MONOXIDE

The fraction W_{r+}/W_{x+}, where $r>x$, is obtained from equations (33) and (36)

$$W_{r+}/W_{x+} \cong \alpha[r-\alpha(r-1)][x-\alpha(x-1)]. \quad (37)$$

If, for example, one sets $x=5$ and $r=19$, equation (37) gives the ratio of the weight of C_{19+} hydrocarbons to the weight of the total liquid plus solid hydrocarbons as a function of α. In general, equation (37) is an expression of the ratio of the weight of the product fraction containing molecules with at least r carbon

atoms to the weight of the product fraction containing molecules with at least x carbon atoms. In figure 70 selected values of W_{r+}/W_{5+} (W_{5+} is total yield of liquids plus solids) are plotted as a function of α ranging from 0.60 to 1.00. For any value of α, the weight fraction for a range of carbon numbers may be read on the plot as the difference in the ordinates of the proper curves. For example, the expected weight fraction in the C_{12}–C_{18} range is the difference in ordinates between the C_{12} and the
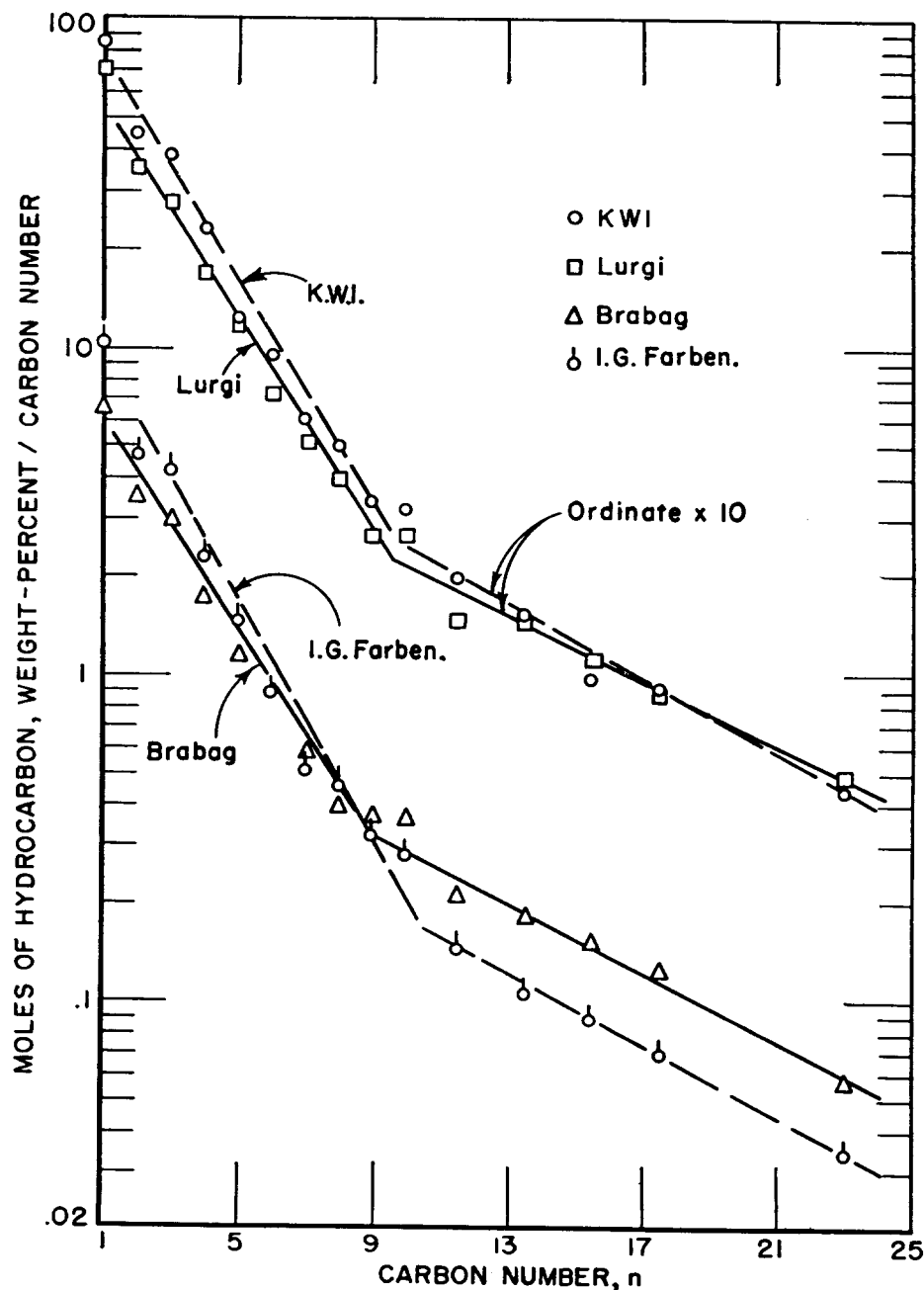
FIGURE 68.—Semilogarithmic Plot of Moles Against Carbon Number for Hydrocarbons From Schwarzheide Experiments.
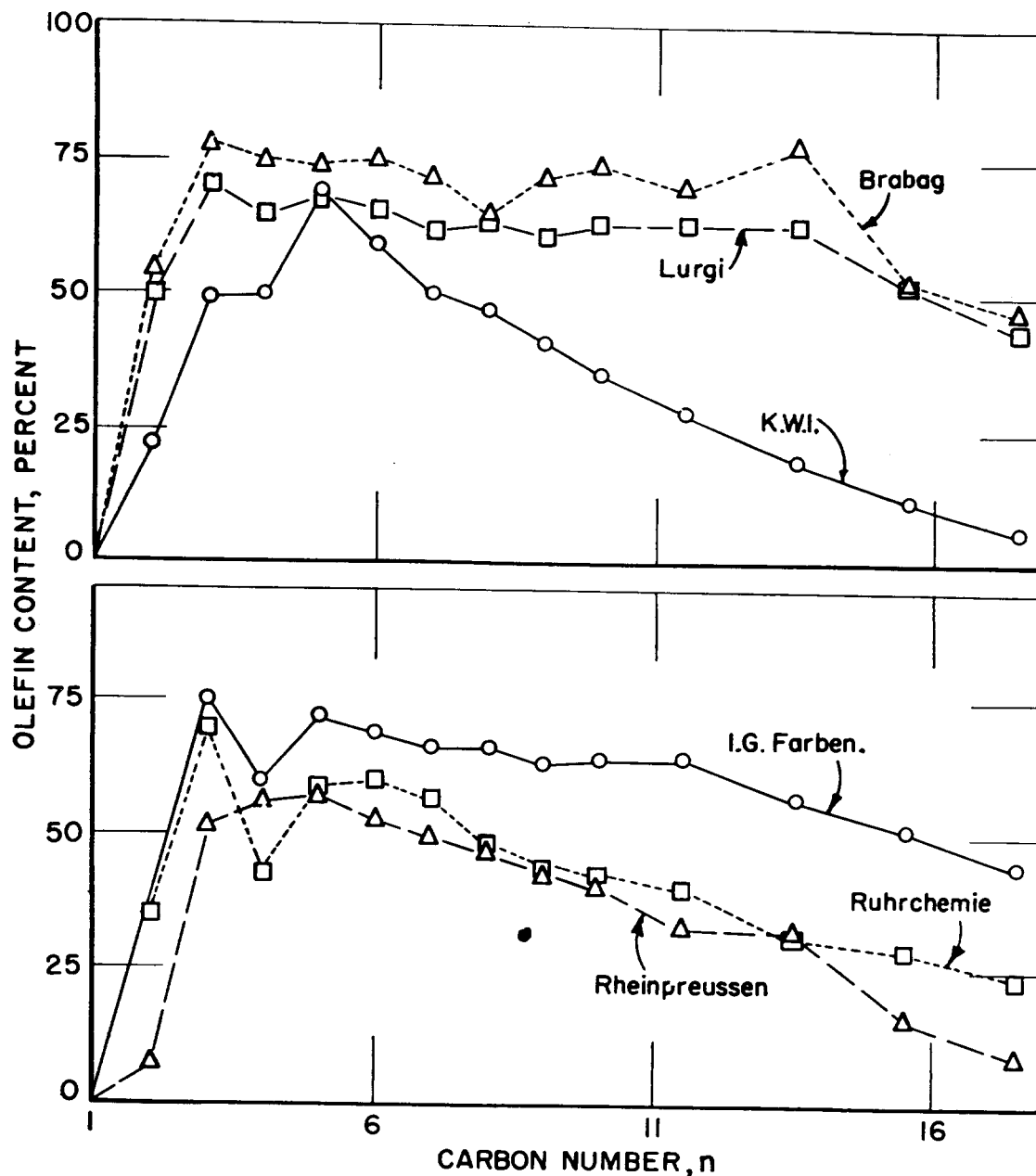
FIGURE 69.—Olefin Content as a Function of Carbon Number for Products From Schwarzheide Experments.

C_{19} curves. If the assumptions are correct, fractionation data on any C_{5+} hydrocarbon product should be consistent with a single value of α. With a plot of this sort, one may use fractionation data derived from as few as three fractions which constitute the total liquid and solid product.

From these calculated curves, the maximum predicted yield of C_{12}–C_{18} diesel oil in the liquid and solid product is about 19 percent. Furthermore, the yield of this fraction goes from 24 percent ($\alpha=0.78$) through a maximum of 29 percent and back to 24 percent ($\alpha=0.92$), that

is, it is not very sensitive to changes in α over a rather wide range. This conclusion may be compared with the following statement by Pichler:[22]

Although by varying pressure, temperature, extent of conversion, and catalyst, it is possible to vary the solid paraffin content of the reaction product considerably, the amount of primary diesel oil cannot be controlled in this way. Comparison of the products * * * showed that the (cobalt) catalyst which contains less kieselguhr and no magnesium favors paraffin. The diesel-oil fractions, on the other hand, showed no

[22] Pichler, H., Synthesis of Hydrocarbons From CO and H₂: Bureau of Mines spec. rept., June 1947, 159 pp.
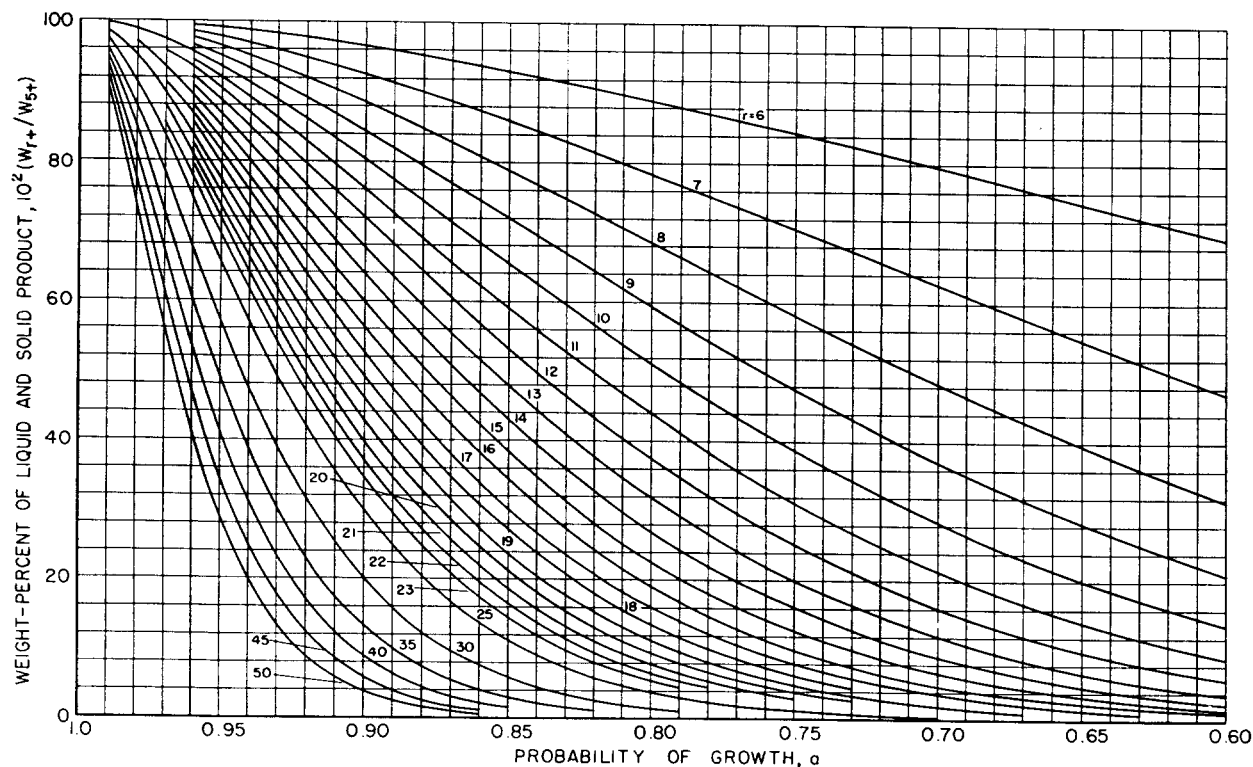
FIGURE 70.—Calculated Product Distributions of Liquid and Solid Fischer-Tropsch Hydrocarbons.

TABLE 67.—Sources for data plotted in figures 71, 72, and 73

All tests in fixed-bed reactors without recycle unless otherwise noted

Figure	Symbol	Catalyst	Operating conditions		Reference
			Pressure, atm.	Temp., °C.	
71	O	Co–Ni	10	190–193	} FIAT reel K21, frames 906–910, 1119–1121
	●	Co–Ni	10	170–190	
	△	Co	10	160–175	} FIAT reel K21, frames 1093–1097.
	▲	Co	10		
	▽	Co	1–151	175–200	Brennstoff-Chem., vol. 11, 1930, p. 489.
	▼	Co	0. 2–7. 0	187–196	TOM reel 36, bag 3451, item 13.
	⊙	Co	¹ 7	204–213	} TOM reel 36, bag 3451, item 1.
	+	Co	¹ 7	190–225	
	×	Co	¹ 7	195–200	TOM reel 37, bag 3450, item 3.
72	O	Fe	² 10	200–225	TOM reel 259, frames 467–654; U. S. Naval Technical Mission in Europe, PB22, 841, Rept. 248–55; BIOS Over-all Rept. 1 (1947) pp. 82–103; TOM reel 134, sec. 1b, item 24.
	●	Fe	³ 15	250–252	FIAT reel K22, frames 1177–1184; reel K31, frames 1108–1115.
	△	Fe	⁴ 20	320–330	FIAT Final Rept. 1267, PB 97, 368.
73	O	Fe	⁵ 7	220–266	} Ind. Eng. Chem., vol. 44, 1952, pp. 395–396.
	●	Fe	⁵ 7	228–280	

¹ Pilot-plant operation with recycle.
² Schwarzheide comparative tests.
³ Slurry operation.
⁴ Hot-gas-recycle operation.
⁵ Alkali content varied.
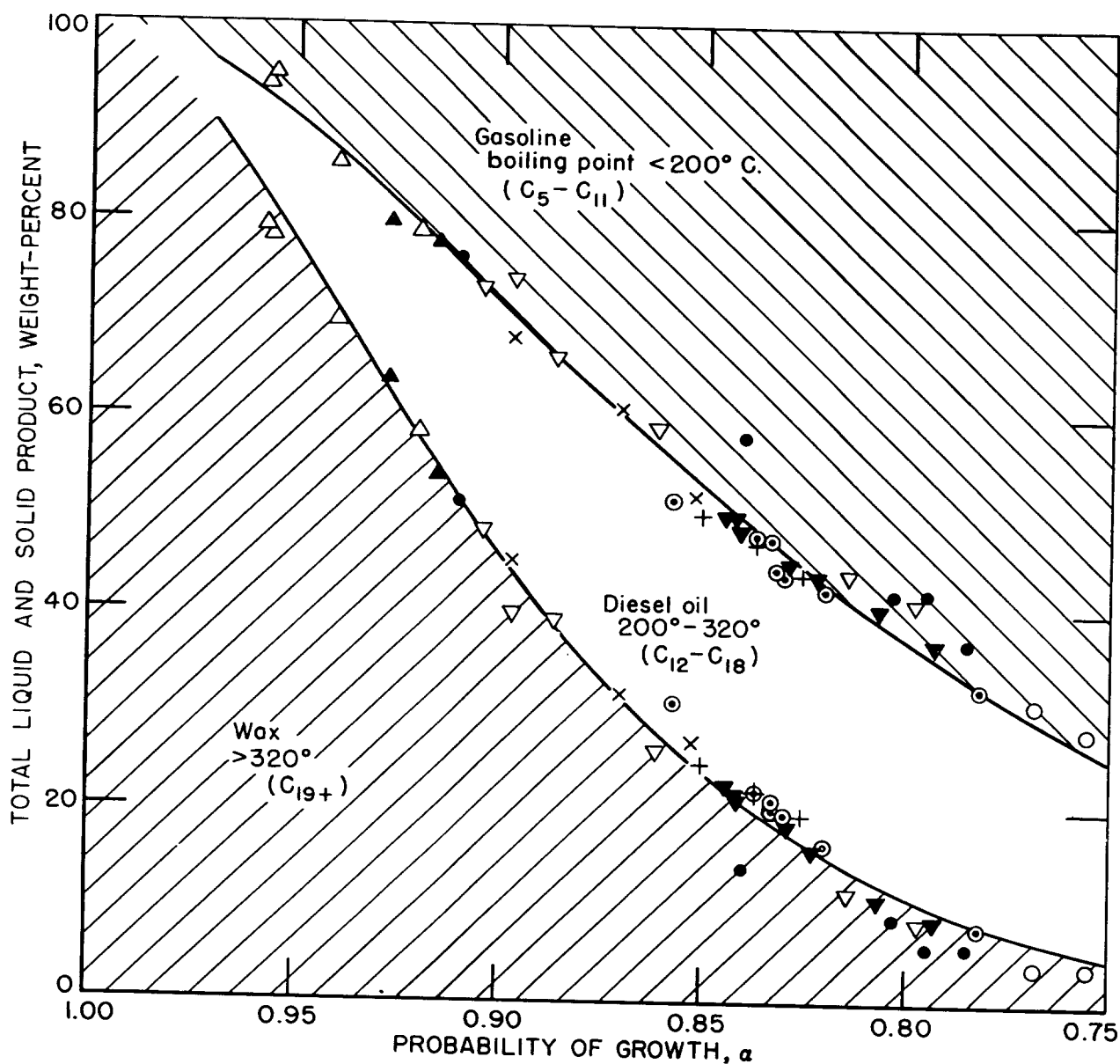
FIGURE 71.—Observed Product Distributions of Liquid and Solid Fischer-Tropsch Hydrocarbons (Cobalt Catalysts), Fitted to Equation (37).

appreciable difference. Experiments with catalysts containing a higher cobalt content gave liquid and solid products containing 50–55 percent of sold paraffin and 25 percent of diesel oil.

The applicability of this method of correlation of product distributions is verified in figures 71 to 73 for iron and cobalt catalysts; the key to these data is given in table 67.

ISOMER DISTRIBUTION

Friedel and Anderson [23] determined the isomer distribution of hydrocarbons from pelleted-cobalt catalyst. Liquid product from

[23] Work cited in footnote 4, p. 112.

one of the catalyst-testing units, employing a cobalt–thoria–kieselguhr (100:18:100) precipitated catalyst at about 190° C. and atmospheric pressure with a space velocity of $1H_2:1CO$ gas of 100 hr.$^{-1}$, was distilled in a 10-plate column and topped at 160°. A 55-cc. aliquot portion of the distillate was percolated through a silica-gel adsorption column in order to separate quantitatively paraffins, olefins, and oxygenated plus other components (table 68). The total paraffin mixture was fractionally distilled into five molecular-weight cuts, C_5–C_8, for analysis of isomers by a Consolidated mass spectrometer. Liquid samples were introduced into the instruments by means of a 0.001-cc. self-filling micro-
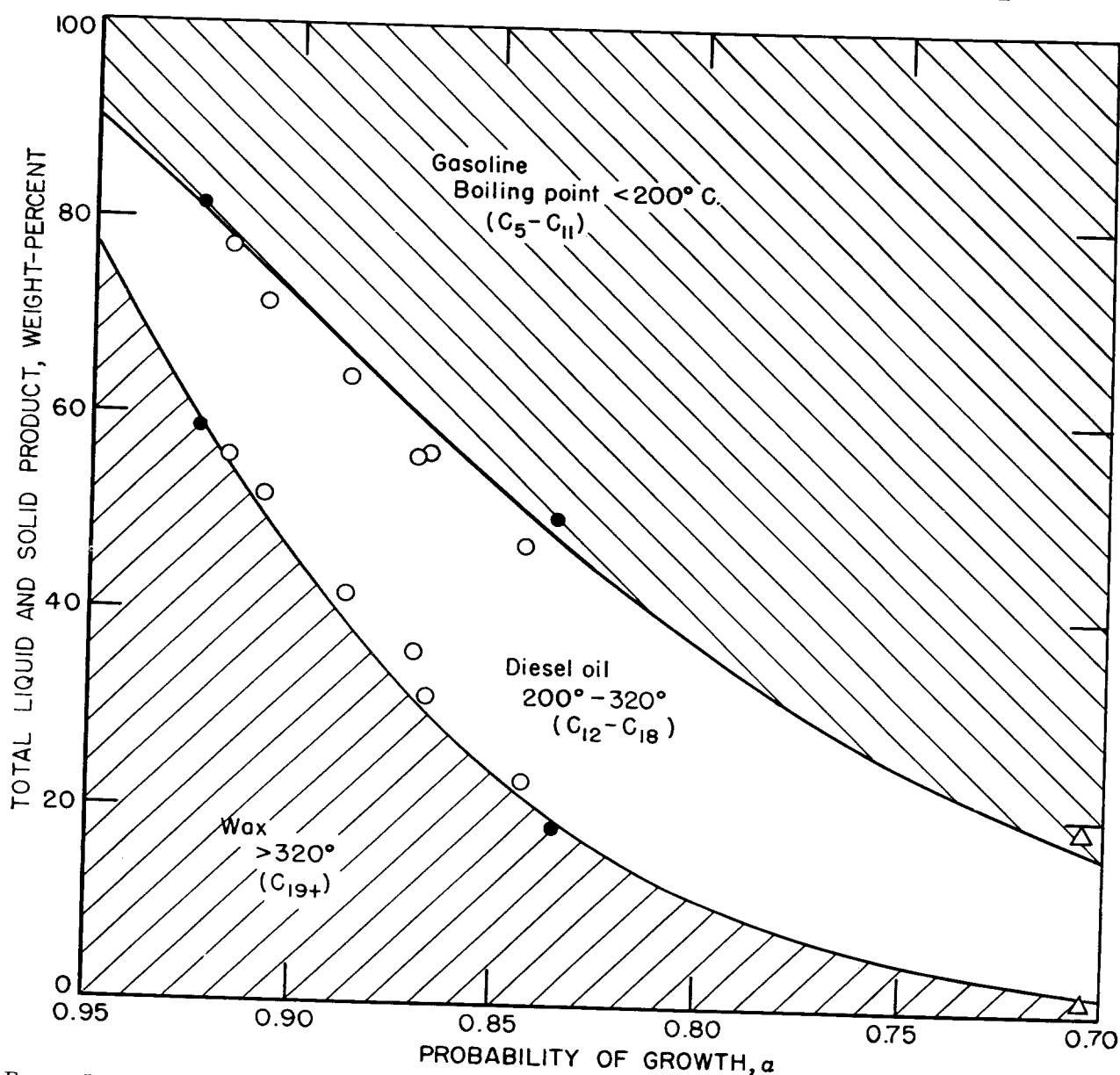
FIGURE 72.—Observed Product Distributions of Liquid and Solid Fischer-Tropsch Hydrocarbons (Iron Catalysts), Fitted to Equation (37).

TABLE 68.—*Fractionation of C_5-C_8 Fischer-Tropsch cobalt-catalyst liquid product by silica-gel adsorption and distillation*

Component:	Volume-percent
Paraffins	71. 7
Olefins	19. 2
Residual (oxygenated material, etc.)	9. 1
	100. 0
Percent of total liquid product	37. 8

pipet.[24] Accuracy was tested in the usual way by analysis of synthetic blends.

[24] Friedel, R. A., Sharkey, A. G., Jr., and Humbert, C. R., Liquid Sampling for Analysis by Mass Spectrometer: Anal. Chem., vol. 21, 1949, p. 1572.

Analyses of paraffin isomers in the C_5-C_8 molecular-weight cuts are given in table 69. Isomeric percentages are given for each C-group on the basis of 100 percent. Of particular interest is the slight but progressive decrease of the straight-chain isomers—the major components—with molecular weight. Von Weber's [25] results predicted this effect but to a greater degree than found in the present work. Results from attempted analyses for various ethyl and dimethyl derivatives are given in table 69 in parentheses. In all instances percentages were very close to zero, being either

[25] von Weber, U., [Determination of Branched Isomers in Mixtures of Paraffin Hydrocarbons]: Angew. Chem., vol. 52, 1939, pp. 607–610.
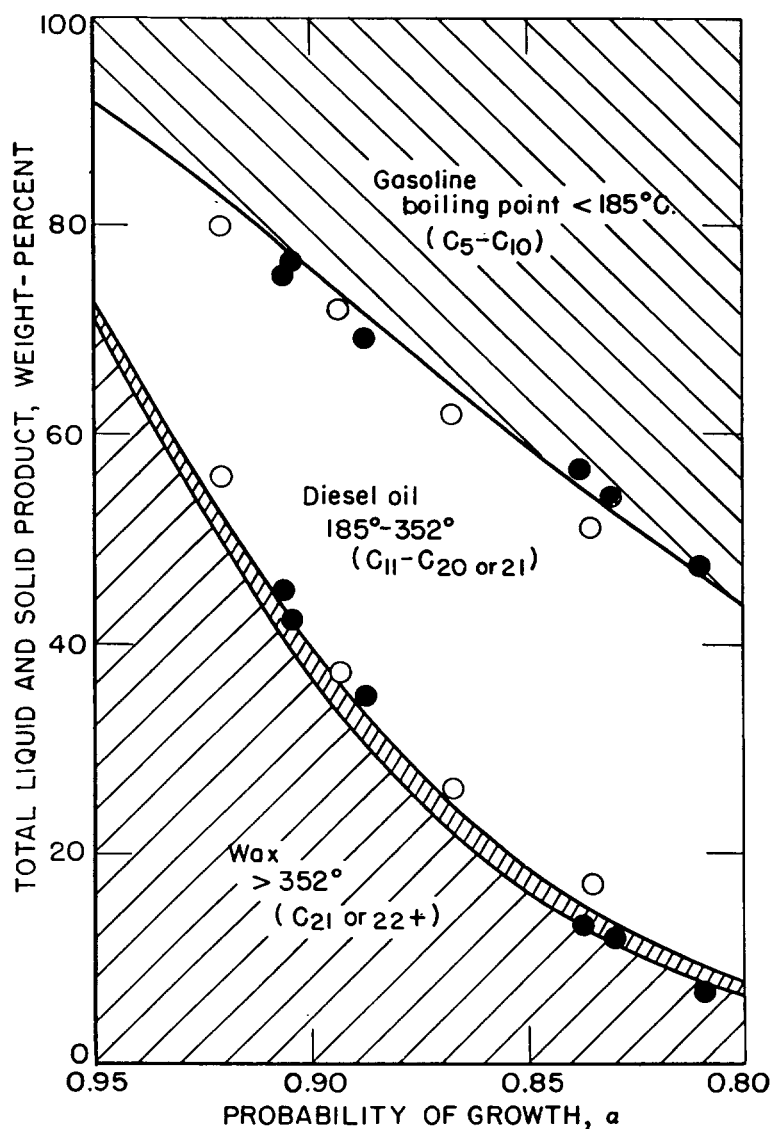
FIGURE 73.—Observed Product Distributions of Liquid and Solid Fischer-Tropsch Hydrocarbons (Iron Catalysts),Fitted to Equation (37).

slightly positive or negative. These data were considered valid evidence for the absence of appreciable concentrations, but did not allow precluding the presence of traces. In these calculations only one isomer containing a quaternary carbon atom—2,2-dimethylbutane—was investigated, and this was found to be absent (−0.4 percent). No indication of this compound or any other of this type has been found.

No detailed analyses of products from iron catalysts have been made as yet at the Bureau of Mines. Data for the isomer distribution from iron catalysts in a fluid-bed system are presented in the next section.

MECHANISM OF CHAIN GROWTH BASED ON ISOMER AND CARBON-NUMBER DISTRIBUTIONS

In the first part of this discussion a chain-growth pattern consistent with observed isomer and carbon-number distributions is considered, and in the second part the growth pattern is described in terms of hypothetical growing groups on the catalyst surface. Several somewhat similar growth patterns have been considered by Weller and Friedel,[26] Anderson, Friedel, and

[26] Weller, S., and Friedel, R. A., Isomer Distribution in Hydrocarbons From the Fischer-Tropsch Process: Jour. Chem. Phys., vol. 17, 1949, pp. 801–803. Isomer Distribution in Fischer-Tropsch Hydrocarbons: Jour. Chem. Phys., vol. 18, 1950, pp. 157–158.

Storch,[27] and Weitkamp and coworkers.[28] However, only the case that most closely corresponds to our postulated reaction mechanism[29] will be considered in this report. In this development it is assumed that

1. Hydrocracking reactions do not occur to a significant extent.

2. Chain growth occurs by stepwise additions of 1 carbon atom to the growing chain.

3. Addition occurs at *only 1 end* of the growing chain on *only 1 end carbon atom* if 2 are present or on the adjacent-to-end carbon.

4. Addition does not occur on an adjacent-to-end carbon already attached to 3 carbon atoms.

5. Rate constants for addition to all end carbon atoms are equal, despite differences in chain length and structure; similarly, rate constants for addition to adjacent-to-end carbons are equal, but different in magnitude from those for end carbons.

Thus, addition to the right end of normal- and iso-C_4 chains with addition at an end carbon (*) or adjacent-to-end carbon (+) may be illustrated as

$$CCC^+C^* \quad \underset{\overline{}}{\overset{2H_2+CO}{\longrightarrow}} \quad \text{Intermediates } (I_i \text{ to } I_n) \rightarrow CCCCC + H_2O, \tag{38}$$

$$\underset{}{\overset{2H_2+CO}{\longrightarrow}} \quad \text{Intermediates } (I_{i'} \text{ to } I_{n'}) \rightarrow \underset{C}{CCCC} + H_2O, \tag{39}$$

$$\underset{C}{CCC^*} \quad \overset{2H_2+CO}{\longrightarrow} \quad \text{Intermediates } (I_{i''} \text{ to } I_{n''}) \rightarrow \underset{C}{CCCC} + H_2O. \tag{40}$$
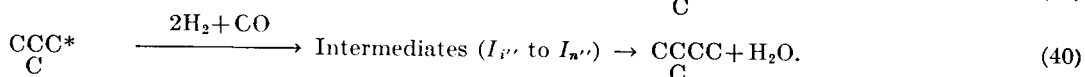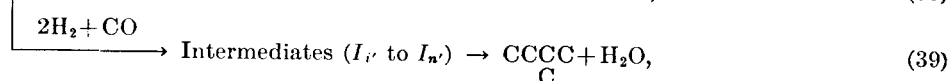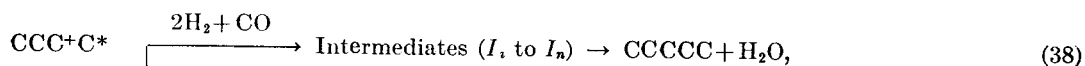
TABLE 69.—*Mass-spectrometer analyses of C_5–C_8 paraffin isomers from Fischer-Tropsch cobalt-catalyst liquid product*

Component:	Composition, volume-percent
C_5s:	
n-pentane	94. 9
Isopentane	5. 1
C_6s:	
n-hexane	89. 6
2-methylpentane	5. 8
3-methylpentane	4. 6
2, 2-dimethylbutane	(−. 4)
2, 3-dimethylbutane	(. 04)
C_7s:	
n-heptane	87. 7
2-methylhexane	4. 6
3-methylhexane	7. 7
3-ethylpentane	(−. 7)
2, 3-dimethylpentane	(−. 02)
2, 4-dimethylpentane	(−. 6)
C_8s:	
n-octane	84. 5
2-methylheptane	3. 9
3-methylheptane	7. 2
4-methylheptane	4. 4
3-ethylhexane	(. 1)
2, 3-dimethylhexane	¹ (Neg.)
2, 4-dimethylhexane	(Neg.)
2, 5-dimethylhexane	(Neg.)

¹ No definite negative percentages can be given because the C_8 results are the summed analyses of 7 fractions.

The reactivity of these carbon atoms may result from the presence of reactive structures, such as an olefin bond, or reactive groups, such as hydroxyl attached to a carbon atom. On addition of carbon monoxide, the growing group passes through a number of intermediate structures indicated by I_i, and eventually forms an intermediate similar to the first but containing an additional carbon atom. From these inter-

mediates molecules, such as aldehydes, alcohols, olefins, or paraffins, may desorb and appear as products.

It is assumed that, upon addition to an end carbon, the rate of growth through intermediates l to n may be represented by a first-order rate constant, α, with respect to the concentration of the growing chain on the catalyst surface; and similarly that, upon addition to an adjacent-to-end carbon, the rate of growth through intermediates l to n may be represented by a first-order rate constant, β. The rate of desorption of the intermediates in both instances is assumed to be characterized by a first-order rate constant, γ, with respect to the concentration of growing chain species. Thus, for chain species, n, the rates of growth by addition to an end or an adjacent-to-end carbon and the rate of desorption are given by αC_n, βC_n, and γC_n, respectively, where C_n is the molar concentration of chain n at the catalyst surface. Therefore, three typical reactions may be considered, with additions occurring at the right end of the chain (reactions (41), (42), and (43)).

$$
\begin{array}{ccc}
CCCC & \rightarrow & CCCC \rightarrow CCCCCC \\
(C_4) & & (C_5) \searrow \\
& & \qquad CCCCC \\
& & \qquad\quad C
\end{array} \tag{41}
$$

$$
\begin{array}{ccc}
CCCC & \rightarrow & CCCC \rightarrow CCCCC \\
(C_4) & & \underset{C}{} \quad \underset{C}{} \\
& & (C_5')
\end{array} \tag{42}
$$

$$
\begin{array}{ccc}
CCCC & \rightarrow & CCCCCC \rightarrow CCCCCCC \\
\underset{C}{} & & \underset{C}{} \searrow \quad C \\
(C_6') & & (C_7') \searrow \\
& & \qquad CCCCCC \\
& & \qquad\quad CC
\end{array} \tag{43}
$$

In steady-state operation the concentration of any species of growing intermediate remains
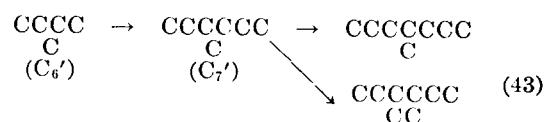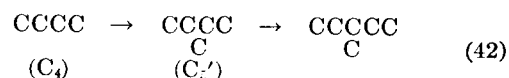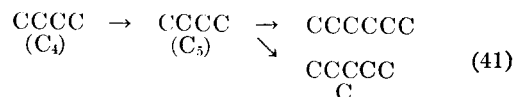
[27] Anderson, R. B., Friedel, R. A., and Storch, H. H., Fischer-Tropsch Reaction Mechanism Involving Stepwise Growth of Carbon Chain: Jour. Chem. Phys., vol. 19, 1951, pp. 313–319.

[28] Works cited in footnote 20, p. 115.

[29] Storch, H. H., Golumbic, N., and Anderson, R. B., The Fischer-Tropsch and Related Syntheses: John Wiley & Sons, New York, N. Y., 1951, 610 pp.

constant; therefore, the rate of formation of a given species must equal its rate of removal by growth and desorption. From the definition of γ, the ratio of the rates of appearance of any two chain species equals the ratio of their concentrations at the surface. Hence, for:

Reaction (41). $C_4\alpha = C_5(\alpha + \beta + \gamma)$
$C_5/C_4 = \alpha/(\alpha + \beta + \gamma) = R_5/R_4 = a.$ (44)

Reaction (42). $C_4\beta = C_5'(\alpha + \gamma)$
$C_5'/C_4 = \beta/(\alpha + \gamma) = R_5'/R_4 = b.$ (45)

Reaction (43). $C_6'\alpha = C_7'\ (\alpha + \beta + \gamma)$
$C_7'/C_6' = \alpha/(\alpha + \beta + \gamma) = R_7'/R_6' = a,$ (46)

where R_n is the rate of appearance of species, n, in moles per unit time, and a and b are constants defined by equations (44) and (45). A new constant, f, defined as $f = b/a$, is introduced. The constant f represents the ratio of the rate of appearance of the isomer formed by addition to an adjacent-to-end carbon to the rate of appearance of the isomer formed by addition to an end carbon atom of a given growing intermediate. In general, for addition to end carbons, $R_{n+1}/R_n = a$; similarly, for addition to adjacent-to-end carbons, $R'_{n+1}/R_n = b = af$.

Starting with a C_2 intermediate and considering all of the possible chain structures that can be formed according to the addition rules, we may evaluate the number of moles in each carbon-number fraction as functions of a and f and the distribution of isomers as functions of f. Specifically, the number of moles in any carbon-number fraction is equal to the number in the C_2 fraction times a function of a and f. It is assumed that both carbon atoms of the C_2 intermediate are effective in end carbon addition, that is, addition characterized by constant a. In table 70 the relative carbon-number distributions are computed with respect to the value of 1 for C_2, and the isomer distribution is evaluated relative to the value of 1 for the normal isomer. To illustrate the method of obtaining the values in table 70, these quantities are derived in detail through C_5 on the basis of the following equations:

$$
\begin{array}{ccccccc}
\text{CC} & \xrightarrow{(1)} & \text{CCC} & \xrightarrow{(2)} & \text{CCCC} & \xrightarrow{(3)} & \text{CCCCC} \\
& & & \searrow & & \xrightarrow{(3')} & \\
& & & & & \searrow & \underset{\text{C}}{\text{CCCC}} \quad (47)\\
& \underset{(2')}{} & & \searrow & & & \\
& & & & \underset{\text{C}}{\text{CCC}} & \xrightarrow{(3'')} & \underset{\text{C}}{\text{CCCC}}
\end{array}
$$

Reaction 1. Both carbons of C_2 are effective in end addition, and R_2 is taken as unity:
Reaction 2. $R_3/R_2 = 2a = R_3$
              $R_4/R_3 = a$
              $R_4 \quad = 2a^2$

Reaction 2'. $R_4'/R_3 = af$
              $R_4' \quad = 2a^2f$
              Total $R_4 = 2a^2(1+f)$
Reaction 3. $R_5/R_4 = a$
              $R_5 \quad = 2a^3$
Reaction 3'. $R_5'/R_4 = af$
              $R_5' \quad = 2a^3f.$
Reaction 3''. $R_5'/R_4' = a$
              $R_5' \quad = 2a^3f$
              Total $R_5 = 2a^3(1+2f).$

It is evident from table 70 that the molar quantity of C_2 is less than that of C_3 for values of a greater than 0.5. When $f=0$, the carbon-number distributions of the present scheme reduce to equation (33) for n greater than 2. The isomer distribution for saturated hydrocarbons from cobalt catalysts [30] (table 69) and data of Bruner [31] for hydrocarbons obtained from iron catalysts were used to test the ability of the expressions in table 70 to predict isomer distribution. Values of f were chosen that appear to give best approximation, and the calculated and experimental data are compared in table 71. For cobalt products the average absolute deviations of normal and monomethyl isomers, in percent, was 1.2, and for products from iron catalysts 1.4. For all cases, the predicted amounts of dimethyl isomers are somewhat greater than those observed. In general, the agreement between predicted and observed isomer fractions is satisfactory, in view of the simplicity of the postulates and the combined errors that are possible in the production and analysis of the products.

From table 70, it is evident that the carbon-number distribution can be expressed by

$$\phi_n = kF_n a^{n-2}, \tag{48}$$

$$\log(\phi_n/F_n) = n \log a + \log(k/a^2), \tag{49}$$

where ϕ_n is the number of moles in the fraction containing n carbon atoms, F_n is the function of f in parentheses in the column marked "Relative carbon-number distribution" in table 70 (that is, for C_7, $F_7 = 1 + 4f + 3f^2$), and k is a constant. Equation (49) is suitable for testing experimental data, since a plot of $\log(\phi_n/F_n)$ against n should be linear. Thus equation (49) satisfactorily expressed the data of figure 67 (p. 115), as f is small for products from cobalt catalysts, this equation is not greatly different from equation (33). However, it was not possible to fit the data shown in figure 68 (p. 116) by a single straight line by using equation (49).

On the basis of the growth pattern just described and the fact that oxygenated molecules appear to be intermediates, Storch, Golumbic, and Anderson [32] postulated a detailed

[30] Friedel, R. A., and Anderson, R. B., Composition of Synthetic Liquid Fuels. I. Product Distribution and Analysis of C_5-C_8 Paraffin Isomers From Cobalt Catalyst: Jour. Am. Chem. Soc., vol. 72, 1950, pp. 1212-1215.
[31] Work cited in footnote 19, p. 115.
[32] Work cited in footnote 29, p. 122.

TABLE 70.—*Isomer and carbon-number distribution in terms of a and f*

	Relative isomer composition	Relative carbon-number distribution, moles
CC	1	1
CCC	1	$2a$
CCCC	1	$\left.\right\}2a^2(1+f)$
CCC / C	f	
CCCCC	1	$\left.\right\}2a^3(1+2f)$
CCCC / C	$2f$	
CCCCCC	1	
CCCCC / C	$2f$	
CCCCC / C	f	$\left.\right\}2a^4(1+3f+f^2)$
CCCC / CC	f^2	
CCCCCCC	1	
CCCCCC / C	$2f$	
CCCCCC / C	$2f$	$\left.\right\}2a^5(1+4f+3f^2)$
CCCCC / CC	$2f^2$	
CCCCC / C C	f^2	
CCCCCCCC	1	
CCCCCCC / C	$2f$	
CCCCCCC / C	$2f$	
CCCCCCC / C	f	
CCCCCC / CC	$2f^2$	$\left.\right\}2a^6(1+5f+6f^2+f^3)$
CCCCCC / C C	$2f^2$	
CCCCCC / CC	f^2	
CCCCCC / C C	f^2	
CCCCC / CCC	f^3	

mechanism for the synthesis. Although many aspects of the synthesis mechanism were not known, these postulates were later shown to be essentially correct by the excellent researches of Emmett and Kummer [33] [34] involving the incorporation of alcohols tagged with carbon-14.

It was assumed that (1) hydrogen is chemisorbed as atoms; (2) carbon monoxide is chemisorbed on surface *metal* atoms, M, in a manner similar to that postulated for the bonds in

metal carbonyls; and (3) the adsorbed carbon monoxide is partly hydrogenated according to equation (50). Chain growth occurs in two ways: (1) By addition to end carbon atoms (equations (51) and (52b)) and (2) by addition to adjacent-to-end carbons (equations (52a) and (53)). The double bonds between carbon and metal atoms are postulated to be more resistant to hydrogenation if the carbon is also attached to a hydroxyl group. Addition at the adjacent-to-end carbon involves partial hydrogenation of the carbon-to-metal bond and follows equations (52a) and (53). Intermediate α is the same as in reaction (51).

TABLE 71.—*Comparison of predicted and observed isomer distributions*

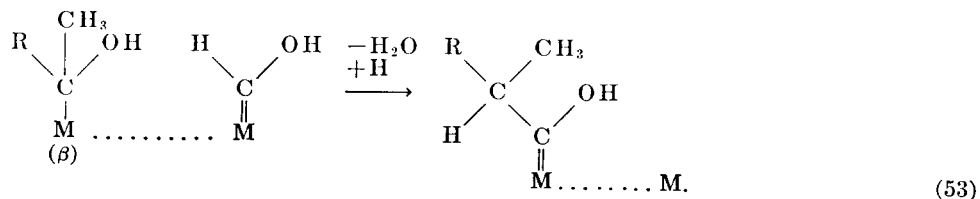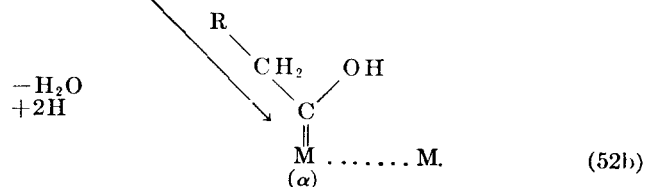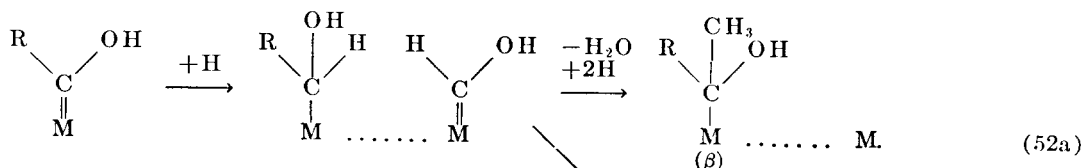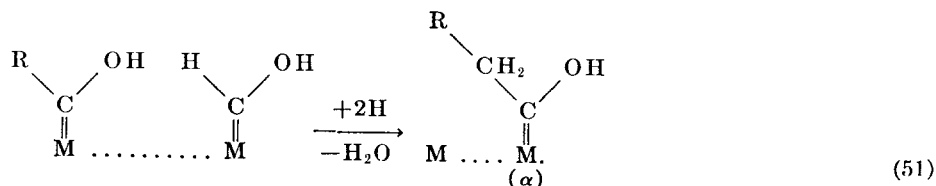|	Isomer distribution, mole-percent			
	Products from cobalt catalysts		Products from iron catalysts	
	Observed [1]	Predicted $f=0.035$	Observed [2]	Predicted $f=0.115$
CCCC	97.0	96.6	89.4	89.7
CCC / C	3.0	3.4	10.6	10.3
CCCCC	95.0	93.4	81.2	81.3
CCCC / C	5.0	6.6	18.8	18.7
CCCCCC	89.6	90.2	78.8	73.5
CCCCC / C	5.7	6.4	11.2	16.9
CCCCC / C	4.7	3.2	9.5	8.5
CCCC / CC	0	.1	.4	.9
CCCCCCC	87.7	87.3	66.0	66.0
CCCCC / C	4.6	6.2	13.1	15.4
CCCCC / C	7.7	6.2	19.1	15.4
CCCC / CC	0	.2	1.6	1.7
CCCC / C C	0	.1	.3	.8
CCCCCCCC	84.5	84.4	61.0	60.5
CCCCCC / C	3.9	6.0		
CCCCC / C	7.2	6.0	36.4	34.7
CCCCCC / C	4.4	3.0		
CCCCC / CC	0	.2		
CCCCC / C C	0	.2		
CCCCC / C C	0	.1	2.6	4.8
CCCCC / CC	0	.1		

[1] From footnote 30, p. 123.
[2] From footnote 19, p. 115.

[33] Kummer, J. T., and Emmett, P. H., Fischer-Tropsch Synthesis Mechanism Studies. The Addition of Radioactive Alcohols to the Synthesis Gas: Jour. Am. Chem. Soc., vol. 75, 1953, pp. 5177–5182.

[34] Kummer, J. T., Podgurski, H. H., Spencer, W. B., and Emmett, P. H., Mechanism Studies of the Fischer-Tropsch Synthesis. Addition of Radioactive Alcohol: Jour. Am. Chem. Soc., vol. 73, 1951, pp. 564–569.

Intermediate β may grow according to reaction (53) to produce a group with methyl side chain. The intermediate may desorb as an aldehyde or be hydrogenated to form an alcohol. The alcohol may dehydrate to an olefin or may dehydrate and hydrogenate to a paraffin. Available data on product distribution indicate a correspondence between C_n hydrocarbons and C_{n+1} alcohols. This fact suggests that the intermediate may decompose to an olefin plus carbon monoxide. These postulated reaction steps with some minor exceptions obey the rules for chain growth described earlier in this section.

$$\begin{array}{ccc} \text{O} & & \text{H}\quad\text{OH} \\ \| & & \diagdown\diagup \\ \text{C} & & \text{C} \\ \| & & \| \\ \text{M}+2\text{H} & \longrightarrow & \text{M.} \end{array} \qquad (50)$$

$$\begin{array}{ccccc} \text{R}\quad\text{OH} & \text{H}\quad\text{OH} & & \text{R} & \\ \diagdown\diagup & \diagdown\diagup & & \diagdown\text{CH}_2\quad\text{OH} & \\ \text{C} & \text{C} & \xrightarrow[-\text{H}_2\text{O}]{+2\text{H}} & \diagdown\diagup & \\ \| & \| & & \text{C} & \\ \text{M} \ldots\ldots\ldots \text{M} & & & \| & \\ & & & \text{M} \ldots \text{M.} & \\ & & & (\alpha) & \end{array} \qquad (51)$$

$$\begin{array}{cccccc} \text{R}\quad\text{OH} & & \text{R}\ \ \overset{\text{OH}}{|}\ \text{H} & \text{H}\quad\text{OH} & \text{R}\ \ \overset{\text{CH}_3}{|}\text{OH} & \\ \diagdown\diagup & \xrightarrow{+\text{H}} & \diagdown|\diagup & \diagdown\diagup & \diagdown|\diagup & \\ \text{C} & & \text{C} & \text{C} & \text{C} & \\ \| & & | & \| & | & \\ \text{M} & & \text{M} \ldots\ldots \text{M} & & \text{M} \ldots\ldots \text{M.} & \\ & & & & (\beta) & \end{array} \qquad (52\text{a})$$

$$\begin{array}{cc} & \text{R} \\ & \diagdown\text{CH}_2\quad\text{OH} \\ \xrightarrow[+2\text{H}]{-\text{H}_2\text{O}} & \diagdown\diagup \\ & \text{C} \\ & \| \\ & \text{M} \ldots\ldots \text{M.} \\ & (\alpha) \end{array} \qquad (52\text{b})$$

$$\begin{array}{cccc} \text{R}\ \ \overset{\text{CH}_3}{|}\text{OH} & \text{H}\quad\text{OH} & & \text{R}\quad\text{CH}_3 \\ \diagdown|\diagup & \diagdown\diagup & \xrightarrow[+\text{H}]{-\text{H}_2\text{O}} & \diagdown\text{C}\diagup \\ \text{C} & \text{C} & & \diagup\quad\diagdown\text{OH} \\ | & \| & & \text{H}\quad\text{C}\diagup \\ \text{M} \ldots\ldots \text{M} & & & \| \\ (\beta) & & & \text{M} \ldots\ldots \text{M.} \end{array} \qquad (53)$$

At present the general aspects of the mechanism of chain growth are understood moderately well, but information regarding the variation of growth constants with catalyst types and operating conditions are lacking. Similarly, few data are available regarding the distribution of a given chain structure into paraffins, olefins, and oxygenated molecules. The kinetics of the synthesis is not well understood, and few reliable data are available. Apparently the synthesis occurs in pores that are largely filled with wax (liquid at synthesis temperatures); and diffusion of dissolved molecules in the liquid phase is directly associated with the reaction at the surface, the latter process producing the concentration gradients required for diffusion. Somewhat more positive are the results demonstrating that bulk carbides are not intermediates in the synthesis.
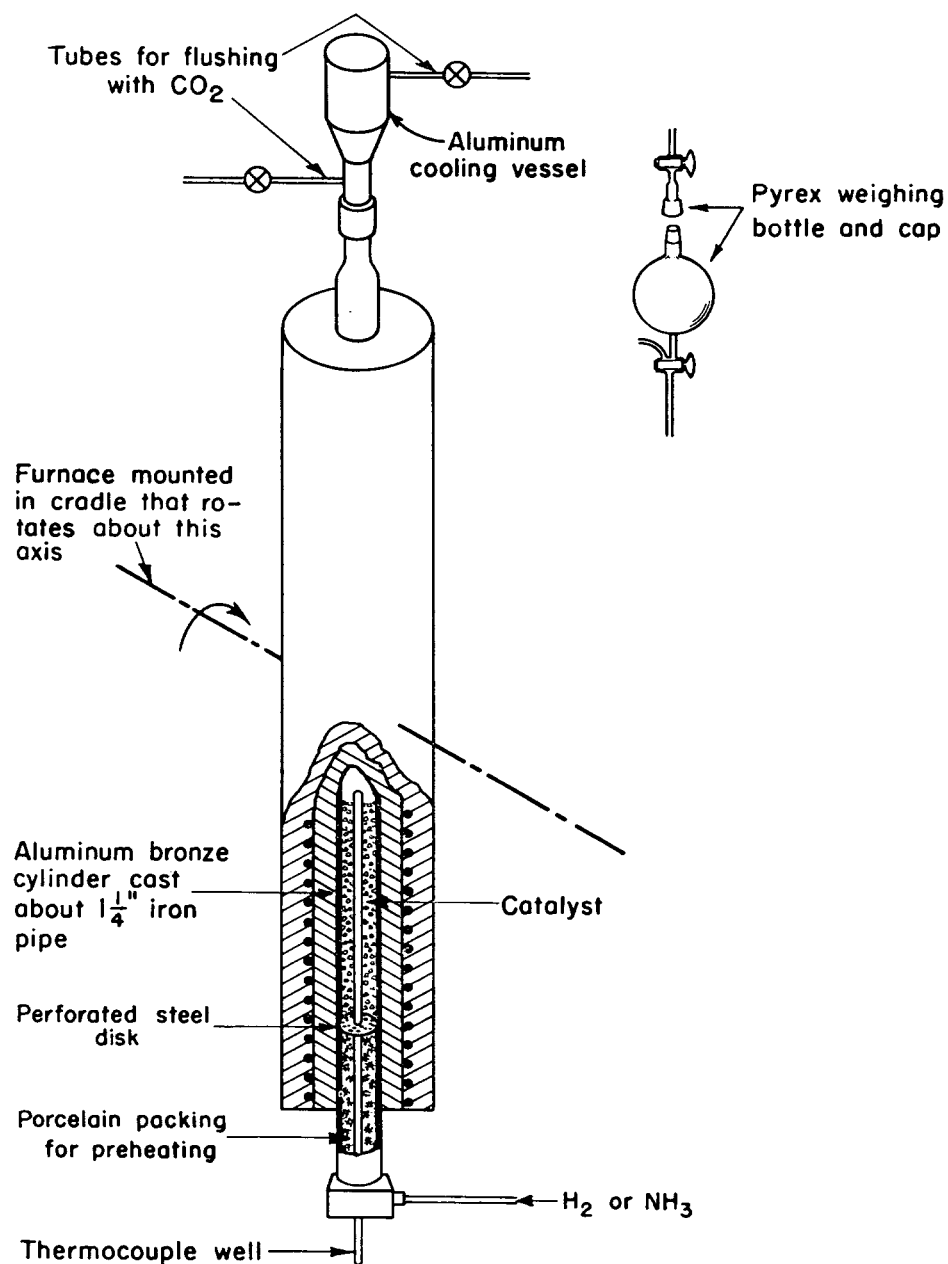
FIGURE 74.—Reduction Unit for Iron Catalysts.

APPENDIX

In the course of these investigations a variety of experimental procedures and apparatus was developed. They have been relegated to this appendix to provide the reader with a moderately detailed description without disrupting the continuity of the presentation of experimental results.

EXPERIMENTAL METHODS FOR PRETREATING IRON CATALYSTS

Iron catalysts are usually pretreated in an electrically heated furnace [35] consisting of an aluminum-bronze block cast about an iron pipe, as shown in figure 74. A simple temperature-control device employed the differential expansion of the heated block and the cradle supporting the reactor tube. With the reactor at temperature and in the position shown in figure 74, the catalyst was placed in the tube in a nitrogen atmosphere. When the catalyst had reached reduction temperature, hydrogen was passed over it at the desired rate. At the end of the reduction period the reactor was rotated 180° and tapped with a hammer, causing the catalyst to fall into the cooling vessel, where it was cooled in hydrogen for about 30 minutes. Carbon dioxide was then passed through the cooling vessel to protect the catalyst from any accidental oxidation in transfer. With carbon dioxide flowing, the cooling vessel was detached, and the catalyst was poured through a rubber sleeve into the glass weighing bottle which was also being flushed with carbon dioxide. This bottle was then closed with its ground-glass cap, and enough carbon dioxide was passed through the cap to remove any air. The bottle plus catalyst was weighed, and the weight was compared with that of the bottle filled with carbon dioxide. After this weighing the catalyst was either charged into the testing units or returned to the reduction furnace for nitriding or carbiding. In transferring the catalyst the following precautions were always taken: (1) The catalyst was kept in a stream of carbon dioxide, (2) no carbon dioxide was passed over the catalyst until its temperature was lower than 50° C., and (3) all transfers were made through rubber or metal connections so that the catalyst was never exposed to air.

Ammonia treatments, either in the reduction unit or with the catalyst in place in the testing unit, were made in a similar manner. Anhydrous ammonia was used without further purification. At the end of the ammonia treatment the catalyst was not permitted to remain in an inert gas or in a slow flow of ammonia, because these conditions favor the hydrogenation or decomposition of the nitride. The catalyst was immediately dropped from the reduction unit; a high flow of ammonia was maintained until the catalyst had cooled below 50° C. The catalyst was then transferred and weighed; usually a weighed sample was removed for X-ray diffraction analysis.

Similar procedures have been developed for preparing Hägg carbide by carburizing a reduced catalyst in carbon monoxide. It is usually desirable to increase the reaction temperature, either stepwise or continuously, to maintain the rate of carbiding approximately constant. This procedure avoids very rapid reaction at the beginning of the pretreatment that causes overheating and oxidation of the iron, and decreases the over-all time required for the pretreatment. Carbonitrides can be prepared by similar methods by either carbiding nitrides or nitriding carbides.

IMPROVED CAUSTIC SCRUBBER

A large-capacity carbon dioxide scrubber,[36] that required changing the caustic solution at 2-week intervals was developed for use with small catalyst testing units for tests with iron catalysts, where it was desirable to remove carbon dioxide from the exit gas. An 8-liter aspirator bottle was used for the scrubber (fig. 75). The gas entered tube A and formed large bubbles in the potassium hydroxide solution at B. These bubbles were broken into smaller ones by scrubbing tubes C; the smaller bubbles passed through and around these tubes as they rose to the surface of the caustic. The rising gas bubbles caused the caustic to circulate from D to E, insuring the availability of fresh solution for absorption on the surface of the scrubbing tubes.

Fabrication of the scrubbing assembly does not require complicated glassblowing, and if necessary the ring seal can be eliminated by

[35] Anderson, R. B., Shultz, J. F., Seligman, B., Hall, W. K., and Storch, H. H., Studies of the Fischer-Tropsch Synthesis. VIII. Nitrides of Iron as Catalysts: Jour. Am. Chem. Soc., vol. 72, 1950, pp. 3502–3508.

[36] Krieg, A., Dudash, A. P., and Anderson, R. B., Improved Caustic Scrubber: Ind. Eng. Chem., vol. 41, 1949, p. 1508.
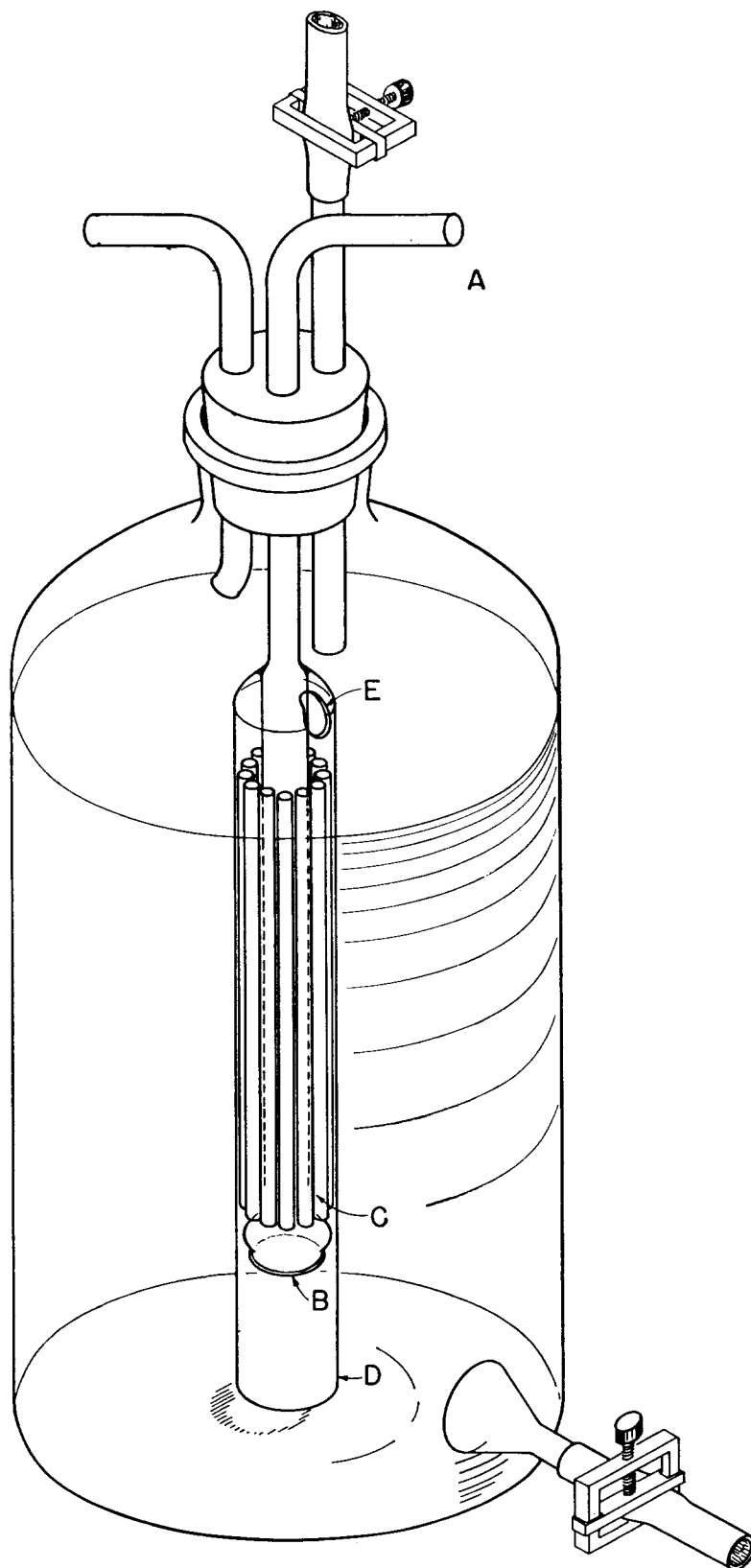
FIGURE 75.—Caustic Scrubber.

supporting tube D on tubes C. The size of the bottle can be varied to any practical limit, because the pressure drop is a function only of the depth of B below the surface which was varied from 8 to 15 cm. without any change in efficiency. In all instances the outer tube of the scrubbing assembly should extend nearly to the bottom of the bottle to insure proper circulation.

As with most other types of caustic scrubbers, it was necessary to use potassium hydroxide rather than sodium hydroxide, since sodium carbonate deposited at point B and eventually stopped the flow of gas. With 40-percent potassium hydroxide solution the scrubber operated efficiently with gas flows as high as 9 liters per hour and carbon dioxide concentrations as high as 35 percent. It probably would operate efficiently at considerably higher flows and carbon dioxide concentrations. With 40-percent potassium hydroxide solution the scrubber operated efficiently for 16 to 21 days with gas containing 35 percent carbon dioxide and flows of 3 liters per hour, which corresponds to 70- to 90-percent conversion to potassium carbonate. In every instance the gas issuing from the scrubber contained less than 0.3 percent carbon dioxide.

GAS-SAMPLING TUBE FOR FIXED-BED REACTOR[37]

The outer tube of the sampling assembly (fig. 76) has ports at 10-cm. intervals along the 90-cm. catalyst bed. By suitable calibration the holes near the end of the snugly fitting inner tube can be placed at any desired port in the outer tube. Gas was slowly withdrawn into the sample-collection system, so that the normal pattern of flow in the reactor would not be altered. This device can only be used for studies at atmospheric pressure.

ADSORPTION AND DENSITY VESSEL

For determination of adsorption isotherms or densities of reduced metal-oxide catalysts it is desirable to reduce the catalyst in the adsorption vessel and to determine the weight loss upon reduction. The adsorption vessel shown in figure 77 has proved convenient in such studies. It is small and light enough to be weighed in an analytical balance. The adsorption vessel consists of a catalyst chamber and a special fourway stopcock.[38] The bores of the stopcock plug are arranged so that both are open in the position shown, while at an angle

of 180° from this position only the right bore is open. The stopcock plug is of hollow-blown construction, and the diameters of bores and capillary tubing are 2 mm. The catalyst chamber is made just large enough to accommodate the sample required, usually 1 to 10 cc. The catalyst chamber is provided with a tube for charging that is closed with a ground joint. The charging tube is equipped with a closely fitting glass tube to decrease the dead space. The tubes leading to the stopcock contain loosely packed wads of glass wool to prevent the catalyst from blowing out of the chamber. The adsorption vessel is connected to the adsorption or reduction system by a 10/30 capillary ground-glass joint.

With the fourway stopcock the sample can be connected to the system for adsorption or evacuation with one bore open; with both bores open a stream of gas such as hydrogen, carbon monoxide, ammonia, etc., can be passed over the catalyst. The catalyst tube is placed in a furnace in a horizontal position to avoid heating the stopcock.

THERMOMAGNETIC ANALYSIS [39-41]

Because of their ferromagnetic characteristics, the carbides of iron are susceptible to thermomagnetic analysis—the study of the temperature dependence of the force experienced by a ferromagnetic substance in an intense, inhomogeneous magnetic field. The temperature at which the force decreases most rapidly with increase in temperature is defined as the Curie temperature or Curie point; it is characteristic of the ferromagnetic phase and serves to identify it. For qualitative information about the known interstitial alloys of carbon and iron, thermomagnetic analysis is superior to chemical analysis, by which no distinction between these alloys can be made as yet. In conjunction with X-ray diffraction and chemical analyses thermomagnetic analysis can be used for quantitative determination of composition and phase changes in catalysts.

The choice of the magnetic field strength is determined by two considerations: (1) The field should be as weak as possible for a clear definition of the Curie points without the introduction of artifacts (qualitative analysis); or (2) it should be as strong as possible to insure that the saturation value of the specific magnetization has been approached over the temperature

[37] Anderson, R. B., Krieg, A., Friedel, R. A., and Mason, L. S., Fischer-Tropsch Synthesis. VI. Differential-Reaction, Rate Studies With Cobalt Catalyst: Ind. Eng. Chem., vol. 41, 1949, pp. 2189–2197.

[38] Anderson, R. B., Improved Adsorption Vessel: Ind. Eng. Chem., anal. ed., vol. 18, 1946, p. 156.

[39] Hofer, L. J. E., Cohn, E. M., and Peebles, W. C., Modifications of the Carbide Fe₂C; Their Properties and Identification: Jour. Am. Chem. Soc., vol. 71, 1949, pp. 189–195.

[40] Hofer, L. J.E., and Cohn, E. M., Thermomagnetic Determination of Hägg Carbide in Used Iron Fischer-Tropsch Catalysts: Anal. Chem., vol. 22, 1950, pp. 907–910.

[41] Cohn, E. M, and Hofer, L. J. E., Mode of Transition From Hägg Iron Carbide to Cementite: Jour. Am. Chem. Soc., vol. 72, 1950, pp. 4662–4663.
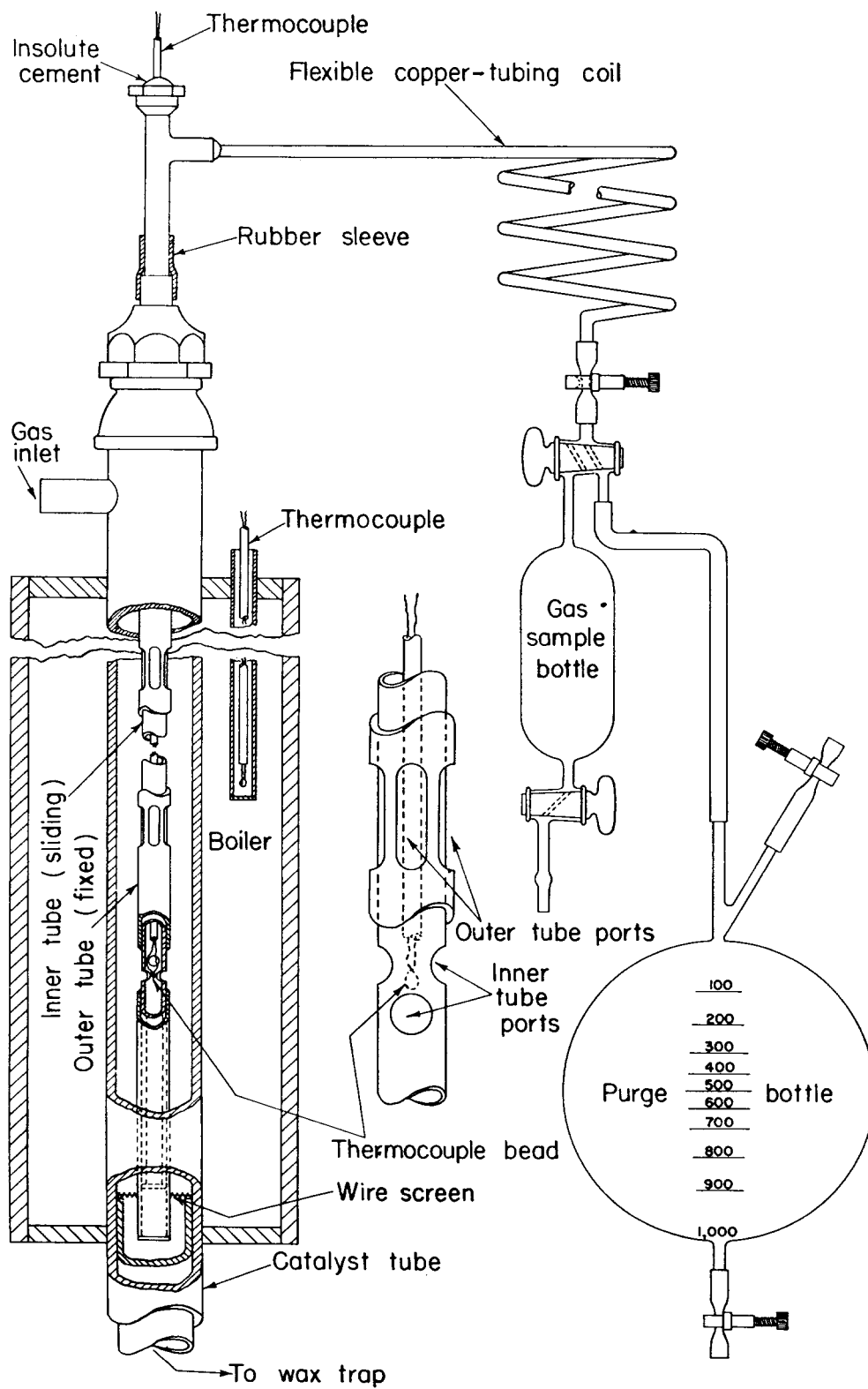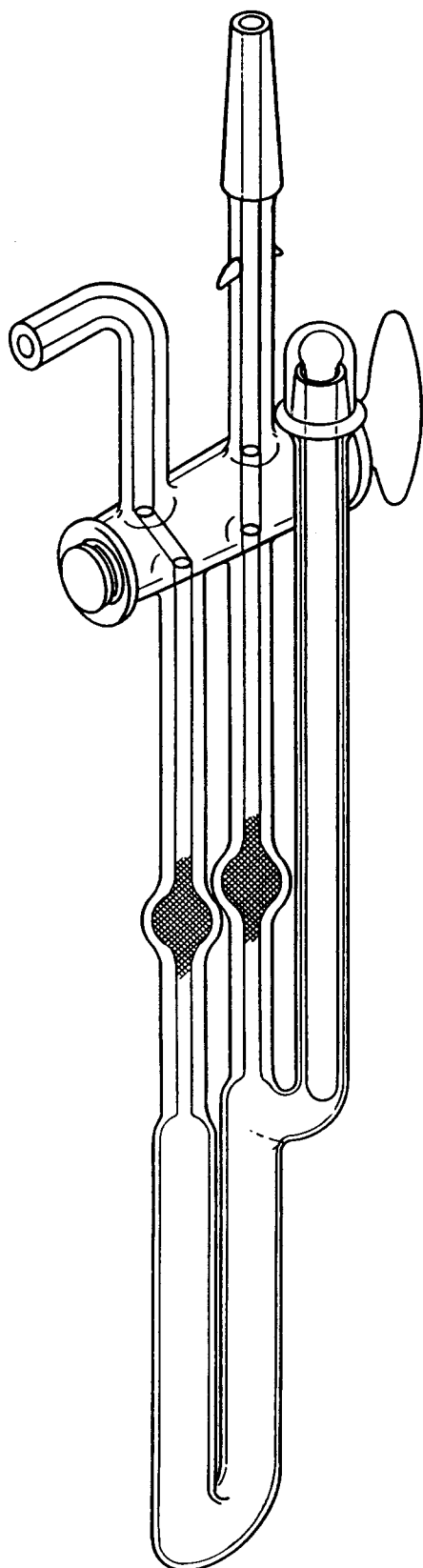
FIGURE 76.—Sampling Device in Converter.

range of the analysis for all ferromagnetic phases present (quantitative analysis). Determinations at either high or low field strength may be carried out, or an intermediate field strength may be used. Thus, an intermediate field strength of about 2,160 gauss has been used by the Bureau of Mines for routine measurements, that being also the limiting safe field strength for continuous, long-time operation of the available small electromagnet. Although the Curie points are not defined as sharply as possible and this field strength is not enough for saturation magnetization, this compromise proved to be satisfactory. The suspension assembly of the magnetic balance is shown in figure 78. For most studies, a strong torsion wire (about 0.1° twist per gram-centimeter torque) was used. A coin-silver cap, provided with a hole and groove on the inside for a thermocouple and its porcelain protective tube, was slipped over the end of the sample holders. This oxidation-resistant cap provided uniform temperature distribution throughout the sample and also identified the temperature of the thermocouple with that of the sample. The junction of the thermocouple was placed as near the sample as possible. Two nonferromagnetic thermocouples have been used—platinum-platinum + 10 percent rhodium or Chromel-Constantan. The use of a ferromagnetic wire, such as Alumel, would superimpose its ferromagnetism upon that of the sample. To insure unrestricted motion of the suspension assembly, the ends of the thermocouple dipped into 2 mercury pools from which 2 wires (identical with those of the thermocouple) led to an ice-bath cold junction. The furnace consisted of an Alundum thimble about 0.9 cm. long and 1.5 cm. I. D., wound noninductively with asbestos-covered 24-gage Nichrome wire and insulated on the outside with a layer of asbestos paper. It was supported between the poles of the magnet by a brass holder and adjusted so that it made no contact with the suspension assembly. In part I of this report [42] the magnet, together with a suspension, has been described.

Samples for magnetic analysis were stored and handled under inert liquids or gases, or in vacuum. When necessary, grinding and thorough mixing were accomplished in a steel mortar partly filled with petroleum ether. Samples of 0.1 to 0.3 gram were transferred to 6- to 9-mm. I. D. Pyrex, borosilicate, or similar tubes (closed at one end and provided with a standard taper joint at the other) held in place with glass wool, evacuated, and sealed under vacuum. The thin sample disks were oriented with their essentially plane sides

FIGURE 77.—Improved Adsorption and Density Vessel.

[42] Storch, H. H., Anderson, R. B., Hofer, L. J. E., Hawk, C. O., Anderson, H. C., and Golumbic, N., Synthetic Liquid Fuels From Hydrogenation of Carbon Monoxide, Part I: Bureau of Mines Tech. Paper 709, 1948, 213 pp.
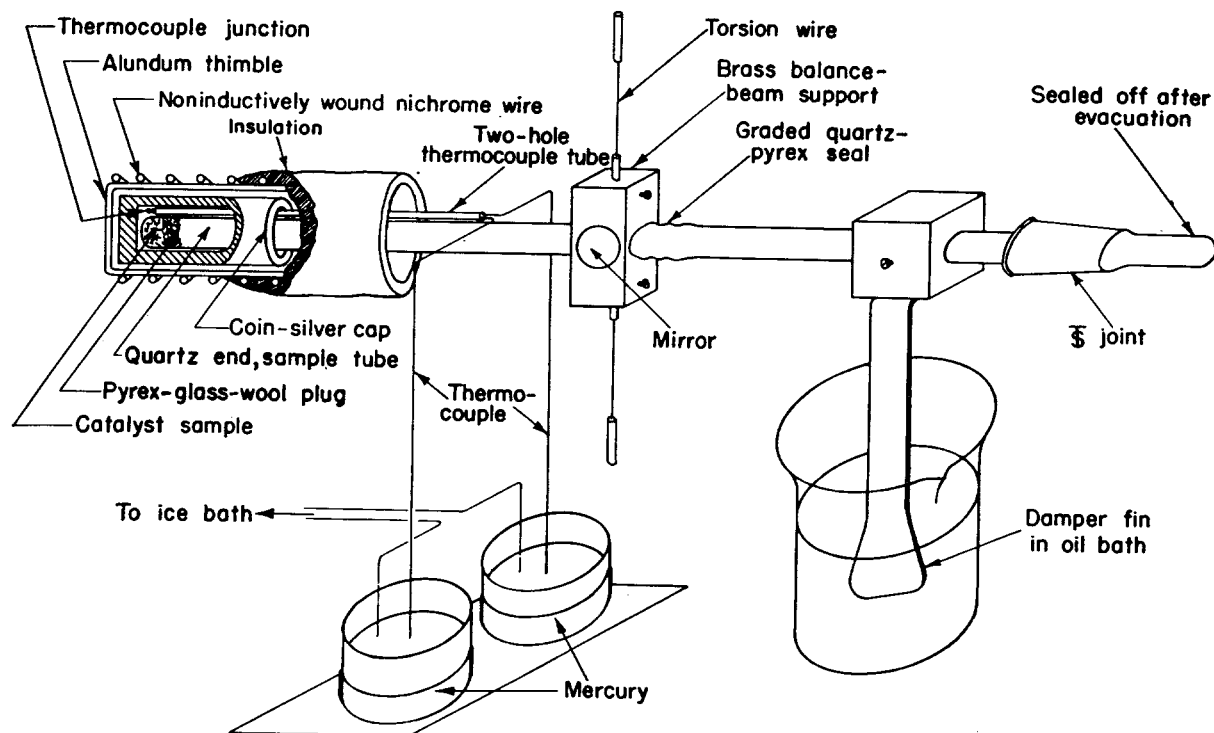
FIGURE 78.—Schematic Diagram of Suspension Assembly With Quartz–Pyrex Sample Tube.
The direction of the field and the field gradient are perpendicular to the plane of the paper.

parallel to the lines of force in the electromagnet, thus minimizing the demagnetization factor.

Hysteresis effects of the torsion wire make it necessary to interrupt the current and to allow the magnetic field to decay after each reading, thus preventing a drift of the null position of the suspension. A small displacement of the sample from null persists after the current is interrupted, unless the apparatus is jarred a number of times. It has been found more convenient to avoid any such mechanical disturbance during analysis. In this way reproducible results can be obtained, and the accuracy of the measurements is not affected seriously.

Because of the reactivity and thermal instability of some of the phases present in used catalysts, the analysis must be carried out fairly rapidly; the heating must be slow enough to avoid temperature gradients between the sample and the point of temperature measurement. Both conditions appear to be fulfilled when used catalysts are heated from room temperature to 530° in 26 to 29 minutes. Cooling curves are seldom characteristic of the original mixture of solid phases because of reactions that have occurred during heating.

Thermomagnetic curves can be evaluated quantitatively only if it is known that no changes take place in the material tested over the range of temperature and time of the anal-

ysis or, if such reactions have taken place, their rates and temperature coefficients are known well enough to make proper allowance for them. It has been found that, in most instances, no serious errors are introduced into the calculations by assuming that no reactions take place in used Fischer-Tropsch catalysts, at least up to 330° C., if fairly rapid heating is employed. Any reactions occurring above that temperature do not interfere with the quantitative analysis of mixtures of Hägg iron carbide, magnetite, and metallic iron, these three phases being the most common ferromagnetic constituents found in used Fischer-Tropsch catalysts. When hexagonal close-packed iron carbide is present with Hägg carbide, the amount of carbide phases can be roughly estimated, but no fully satifactory method for quantitative determination has been developed as yet.

The thermomagnetic curves for the various phases in a mixture are simply additive, and each phase exhibits a magnetic moment that is the product of its specific magnetization and its mass. Thus, figure 79 represents an ideal thermomagnetic curve of a mixture of equal amounts of magnetically saturated metallic iron, magnetite, and cementite. It was constructed from experimental thermomagnetic curves by arbitrarily neglecting the paramagnetic contribution to the magnetic moment near the Curie point and eliminating the low-